

# Propagation Characteristics of $2\text{H}_2/\text{O}_2/2\text{Ar}$ Detonations in Channels with Constant Area Divergence

<sup>a</sup>Qiang Xiao, <sup>b</sup>Jiixin Chang, <sup>a</sup>Maxime La Fleche, <sup>c</sup>Yongjia Wang, <sup>a</sup>Matei I. Radulescu

<sup>a</sup> Department of Mechanical Engineering, University of Ottawa, Ottawa, Canada

<sup>b</sup>Faculty of Applied Science and Engineering, University of Toronto, Toronto, Canada

<sup>c</sup>School of Power and Energy, Northwestern Polytechnical University, Xian, China

## 1 Introduction

Ideally, detonations in gases are considered to propagate steadily at CJ speed while neglecting any other non-ideal effects, such as mass divergence, friction, and heat loss. These losses in reality would result in detonation attenuation characterized by propagation velocity deficit and to some extent even detonation failure. As is the main loss mechanism for detonation attenuation and possible extinction [1], mass divergence in general could result from two types, namely, the lateral flow divergence in the reaction zone and the geometrical area divergence. The first type involves detonation propagation in narrow channels or tubes which render the divergence of reacting gases into the viscous boundary layers that act as a mass sink to the core flow, and in leaky or porous wall tubes which could also lead to lateral flow divergence. The second case usually happens in detonation diffraction with abrupt area changes. Although a lot of works have been done on attempting to relate the detonation velocity with the mass divergence in porous wall tubes [2, 3] or in narrow channels or tubes [4–6], a number of assumptions have been used, which probably could result in a significant impact on the predictions. It is difficult to make a precise quantification of the mass divergence in the above frameworks.

Very recently, Borzou and Radulescu [7,8] formulated a solution allowing for an easy and precise quantification of loss effects during detonation propagation involving an exponentially shaped channel. The constant logarithmic derivative of the cross-sectional area not only enables detonations to propagate with a constant mass divergence but also allows the visualization of the evolution process by Schlieren and Shadowgraph techniques. From the comparison, they found that the detonation dynamics departed from the ZND model predictions, particularly for very unstable detonations. Thus, the question arises if the ZND model can predict the dynamics of much less unstable mixtures, in spite of the presence of a cellular structure. To answer it, the present study aims to extend this technique to a more stable mixture of  $2\text{H}_2/\text{O}_2/2\text{Ar}$  with better known kinetics to understand the propagation characteristics.

## 2 Experimental Setup

Figure 1 presents the schematic of the shock tube for all the experiments involved in this study. It was a 3.4 m long aluminium rectangular channel with an internal height and width of 203 mm and 19 mm, respectively. It comprises three sections, a detonation initiation section, a propagation section, and a test section. The mixture was ignited in the first section by a high voltage igniter (HVI), which could store up to 1000 J with the deposition time of 2  $\mu\text{s}$ . Mesh wires were inserted in the initiation section for promoting the formation

of detonations. Eight high frequency piezoelectric PCB pressure sensors ( $p_1$ - $p_8$ ) were mounted flush on the top wall of the shock tube to record pressures and measure propagation speeds. The exponentially designed divergent ramp was placed in the test section, which was equipped with two glass panels for the visualization purpose. Two polyvinyl-chloride (PVC) ramps with different area divergence rates were tested for validating the boundary layer losses rendered by the channel. The long ramp was about 1.0 m in length with the rate of  $2.3 \text{ m}^{-1}$ , while the short one was 0.5 m in length with the rate of  $4.6 \text{ m}^{-1}$ . The initial gap between the ramp tip and the top wall of the channel is 23 mm in height. The mixture presently studied was  $2\text{H}_2/\text{O}_2/2\text{Ar}$ . It was prepared in a separate mixing tank by the method of partial pressures and was then left to mix for more than 24 hours. Before filling with the test mixture in every single experiment, the whole channel was evacuated to below the absolute pressure of 90 Pa. A driver gas of  $\text{C}_2\text{H}_4/3\text{O}_2$  separated by a diaphragm was used in the initiation section when the initial pressure was lower than 10.3 kPa. For visualizing the detonation evolution process along the exponential ramp, a large-scale shadowgraph technique by using a  $2\text{m}\times 2\text{m}$  retro-reflective screen with a Xenon arc continuous light source of 1600 W was adopted. The resolution of the high-speed camera is  $1152\times 256$  with the frame rate of 42496 fps. The exposure time is set to  $2.0 \mu\text{s}$ . More than 100 experiments were performed for initial pressures in the range of 2.5 kPa-41.5 kPa and initial temperature of 298 K.

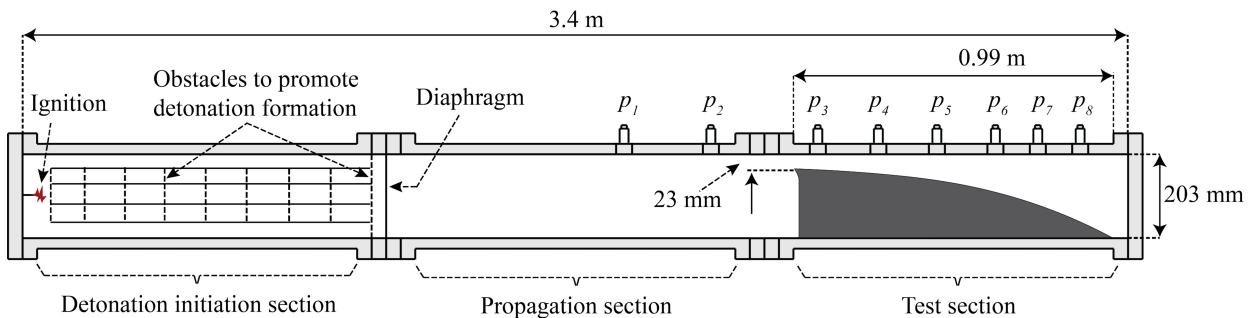


Figure 1: Schematic of the shock tube.

### 3 Results and discussion

#### 3.1 Experimental Results

Figures 2 (a), (b), and (c) show the superposition of shadowgraph photos of detonation fronts propagating along the divergent ramp at different time for three different initial pressures. All the fronts in each superimposed graph were taken from the same experiment. At sufficiently high pressures, like 14.82 kPa as shown in Fig.2 (a), detonation fronts are uniformly curved with fine cellular structures. Despite the mass divergence rendered by area expansions, leading shocks are still so closely coupled with the trailing reaction fronts that no distinctive unreacted pockets and induction zones could be clearly seen. The uniform average spacing of triple points along detonation fronts indicates that the generation rate of new cellular structures is comparable to the area divergence rate and that detonation could be assumed to be quasi-steady while propagating along the large divergent ramp.

By decreasing the initial pressure for lowering the sensitivity of mixtures, area divergence plays a more significant role. Detonation fronts tend to demonstrate behaviors like local decoupling of reaction fronts from leading shocks and consumption of the unreacted induction zones behind leading shocks by transverse waves, which could be easily seen from Figs.2(b) and (c). Compared to that of the higher pressure of 14.82kPa in Fig.2 (a), the growth rate of triple points is much lower in Fig.2 (b) and (c), and does not match the area divergence rate. For example, despite the area increase due to divergence, the number of triple

points in Fig.2 (b) does not increase until detonation fronts propagate to about 3/4 ramp length (see Frame 20). More interestingly, when the pressure decreases to the critical one of 5.52kPa, below which detonations decouple completely, detonations could successfully travel with only one triple point. Previous works proposed the onset of single-headed spinning detonations as a criterion for propagation limits for detonations in round tubes and thin annular channels [9, 10]. Here, it further shows that single-headed detonation also exists in the large thin channel near the pressure limit for detonation propagation.

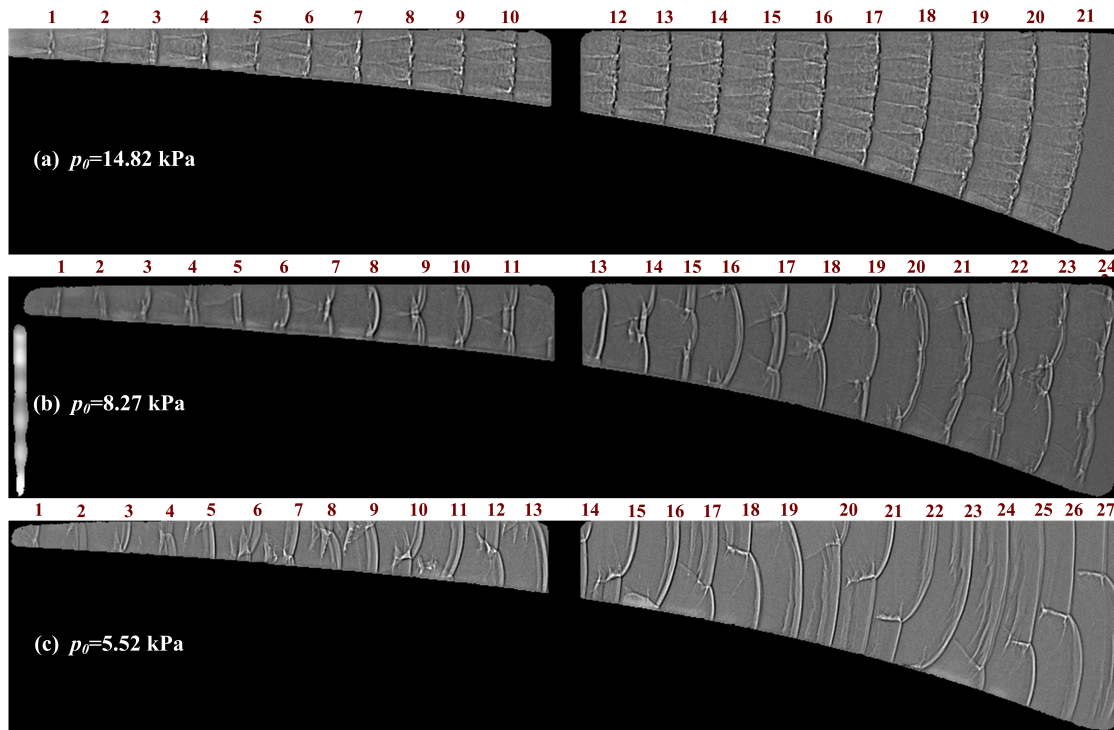


Figure 2: Superposition of detonation fronts at different time for different initial pressures.

The other interesting point involves the role of transverse waves in propagation of regular cellular detonations. There is a misconception that transverse waves in such argon diluted mixtures are weak, whereas they have been known to be much stronger than in unstable detonations since the pioneering works of Subbotin [11], Strehlow and Biller [12], and Edwards et al. [13], who measured the strength of the transverse waves. Although it is difficult to pinpoint the role of transverse waves like igniting unreacted mixtures behind the leading shock in high pressures, as demonstrated in Fig.2 (a), due to the small spacing of transverse waves and also the complete coupling between leading shocks and following reaction fronts. Even possibly, leading shocks are strong enough to ignite all fresh mixtures upstream. However, when initial pressures approach the critical one for detonation propagation, transverse waves are reactive to ignite the unreacted shocked gases that exist in induction zones, which could be seen from Fig. 2(b) and (c). Especially for the limit pressure of Fig. 2(c), distinctive transverse detonation is generated for combusting the unreacted mixtures. Figures 3(a) and (b) show the detailed transverse wave structure, which is not fully demonstrated in Fig. 2(c). It consists of two parts, a reactive one connected to the triple point and the other nonreactive one that extends far behind. The reactive part, i.e., transverse detonation, is strong enough to periodically consume the unreacted zones behind the incident shock, thereby providing energy feedback to the leading

shock. This constitutes a possible mechanism for near-limit detonation propagation. Figure 4 shows veloc-

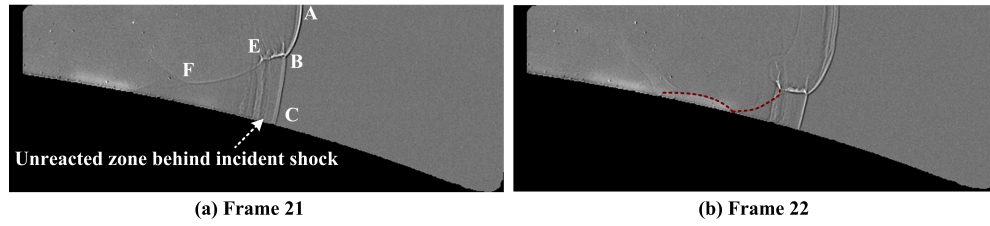


Figure 3: Shadowgraph photos of (a) Frame 21 and (b) Frame 22 for pressure of 5.52 kPa, AC: Leading shock, BE: The reactive part of transverse wave (transverse detonation), EF: The nonreactive part of transverse wave.

ity profiles of detonation fronts for initial pressures of  $p_0=8.27$  kPa and  $p_0=5.52$  kPa. It could be seen that, despite the fact that the propagation speed could vary from  $0.5\sim 0.7 D_{CJ}$  to  $1.0\sim 1.1 D_{CJ}$ , the averaged propagation speed in each cellular cycle could be considered constant. This means that the quasi-steady assumption would still be applicable to near-limit pressures for detonations propagating along the large ramp with constant area divergence so that averaging of the global propagation speed would be meaningful. Due to mass divergence rendered by area expansion and boundary layer effect, the globally averaged speed is smaller than CJ speed.

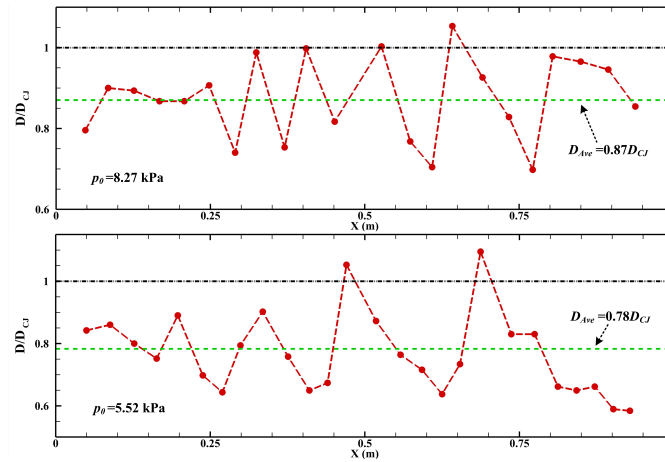


Figure 4: Velocity profiles (along the top wall) of detonation fronts for  $p_0=8.27$  kPa (top) and  $p_0=5.52$  kPa (bottom).

### 3.2 Comparison of the experimental $D - K_{eff}\Delta_i$ relationship with ZND predictions

In order to quantitatively investigate dynamics of detonations propagating along the large ramp with constant area expansion, globally averaged speeds were calculated from each experiment. For the purpose of validating the part of mass divergence due to boundary layers, additional experiments of detonations in channels with small ramp and without ramps were both conducted. Averaged propagation speeds were correspondingly computed from each experiment. Figure 5 shows the comparison of the experimental  $D - K_{eff}\Delta_i$  relations with that predicted by the generalized ZND model which takes mass divergence into account.  $K_{eff}\Delta_i$  is the non-dimensional rate of mass divergence, where  $\Delta_i$  is the ZND induction length calculated

by using Shepherd's SDToolbox [14] and  $K_{eff}$  is the effective rate of mass divergence due to both the constant area expansion and the boundary layer impact. Borzou [8] estimated the equivalent mass divergence due to boundary layers of the geometrical channel by collapsing the experimental data of two ramps with different divergence rate and found that the equivalent mass divergence of boundary layers is  $5.5 \text{ m}^{-1}$ . In this study, experimental results in channels without ramps were also adopted for further validating the equivalent mass divergence of boundary layers. The  $D - K_{eff}\Delta_i$  data show that results of the three different series of experiments collapse pretty well for high pressures. This means that the mass divergence of  $5.5 \text{ m}^{-1}$  due to boundary layers still applies to the present study.

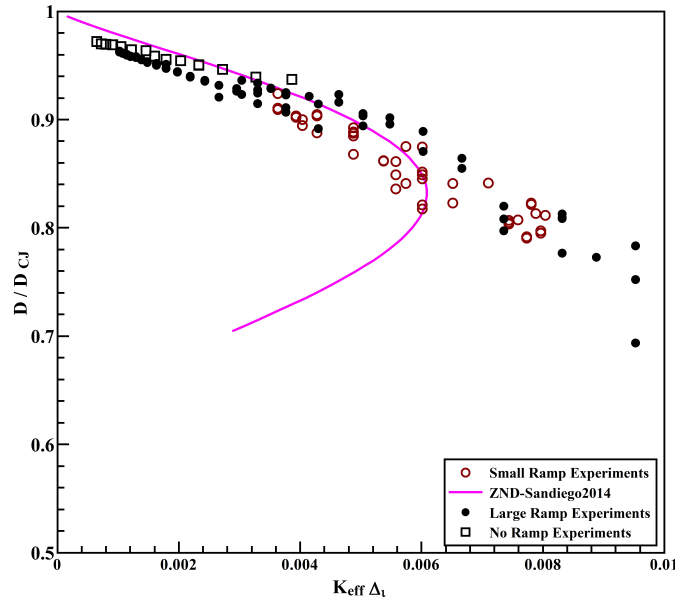


Figure 5: Comparison of the experimental  $D - K_{eff}\Delta_i$  relations with ZND predictions.

By solving the ordinary differential equations (ODEs) of the generalized ZND model that includes mass divergence, the predicted  $D - K_{eff}\Delta_i$  curve could be obtained as shown in Fig.5. The details of calculating this set of ODEs could be found in Refs. [1, 15]. The Sandiego2014 mechanism was utilized for describing reaction kinetics. From the comparison, it could be seen that, the generalized ZND model with mass divergence could excellently predict the experimental results for moderate divergence and small velocity deficits despite its under-prediction of the limiting mass divergence. In experiments, the critical mass divergence for detonation failure is  $\sim 0.01$ , while the predicted one is  $\sim 0.006$ . A possible explanation for this discrepancy could be attributed to the role of reactive transverse waves near the limit for detonation propagation. As shown in previous section, transverse detonations consume the unburnt mixtures behind leading shocks and release energy to sustain the leading shock. On the other hand, the 1-D generalized ZND model neglects the effects of transverse waves. Thus, this promotion effect exerted by transverse detonations favorably extends the critical mass divergence to a lower one compared to the theoretical one predicted by the model.

#### 4 Conclusion

In the present study, propagation of  $2\text{H}_2/\text{O}_2/2\text{Ar}$  detonations with constant area divergence has been experimentally investigated. The propagation characteristics of detonation propagation along the large ramp in a wide range of pressures has been demonstrated and analyzed. The results show that quasi-steady detonations could be assumed for this study so that averaging of global propagation speeds is reasonable for getting

the  $D - K_{eff}\Delta_i$  relationship. Near the limit, transverse waves are found to be reactive for consuming the unreacted mixtures behind leading shocks. At the critical pressure, single-headed detonations travel with transverse detonations, whose maximum speed could reach the CJ value. The promotion effect by reactive transverse waves probably accounts for the failure of the generalized 1-D ZND model to predict the limiting mass divergence, and it can be speculated that these transverse detonations provide the mechanism for promoting the propagation of the cellular detonations. Despite the discrepancy, experimental results are in excellent agreement with the predictions for moderate divergence and small velocity deficits.

## References

- [1] R. Klein, J.C. Krok, and J.E. Shepherd.(1995). GALCIT Report FM 95-04.
- [2] Radulescu, Matei I., and John HS Lee.(2002) *Combustion and Flame* 131.1: 29-46.
- [3] Mazaheri, Kiumars, et al.(2015).*Combustion and Flame* 162.6: 2638-2659.
- [4] Chao, J., et al.(2009). *Proceedings of the Combustion Institute* 32.2: 2349-2354.
- [5] Camargo, Alexandra, et al. (2010). *Shock Waves* 20.6: 499-508.
- [6] Gao, Yuan, et al.(2016). *International Journal of Hydrogen Energy* 41.14: 6076-6083.
- [7] Borzou B., et al. *Proceedings of the 25th international colloquium on the dynamics of explosions and reactive systems*. Leeds, UK. 2015.
- [8] Borzou, Bijan. (2016). PhD Thesis. University of Ottawa.
- [9] Lee, John HS, et al.(2013). *Proceedings of the Combustion Institute* 34.2: 1957-1963.
- [10] Moen, I. O., et al. (1981). *Symposium (International) on Combustion*. Vol. 18. No. 1.
- [11] Subbotin, V. A. (1975). *Combustion, Explosion and Shock Waves* 11.1: 83-88.
- [12] Strehlow, Roger A., and John R. Biller.(1969). *Combustion and Flame* 13.6: 577-582.
- [13] Edwards, D. H., et al. (1970). *Astronautica Acta* 15.5: 323-333.
- [14] <http://shepherd.caltech.edu/EDL/public/canera/html/SDToolbox>
- [15] Radulescu, Matei Ioan. (2003). PhD Thesis. McGill University.